An Integrated Traction and Compressor Drive System for EV/HEV Applications

Gui-Jia Su and John S. Hsu
National Transportation Research Center
Oak Ridge National Laboratory
2360 Cherahala Blvd., Knoxville, TN 37932
sugj@ornl.gov

***Abstract*— This paper presents an integrated traction and compressor drive to reduce the HVAC compressor drive cost in electric and hybrid electric vehicle (EV/HEV) applications. The drive system employs a five-leg inverter to drive a three-phase traction motor and a two-phase compressor motor. The common terminal of the two-phase motor is tied to the neutral point of the three-phase traction motor to eliminate the requirement of a third phase-leg. The cost of the compressor drive can be significantly lowered due to the elimination of one phase-leg and additional part count reduction made possible by sharing the switching devices, dc bus filter capacitors, gate drive power supplies, and control circuit. Simulation and experimental results are included to verify that speed control of the two motors is independent from each other.**

Keywords-EV/HEV traction drive; EV/HEV compressor drive; five-leg inverter; two-phase motor; zero-sequence current

I. INTRODUCTION

Because of their superior performance over the conventional engine belt-driven counterparts, electric motor driven compressors for heating, ventilating, and air-conditioning (HVAC) are being deployed in automobiles with a 42V power net and hybrid electric vehicles (HEVs) where a high-voltage bus is readily available [1-4]. The advantages of electrically driven HVAC compressors include: (1) highly efficient operation as the compressor speed can be adjusted according to the cooling/heating requirements, but independent of engine speed unlike the conventional belt driven compressor; (2) flexible packaging as the installation location is not restricted to the accessory drive side of the engine; and (3) reduced leakage of the refrigerant into the atmosphere because of the elimination of the rotating seals [4]. In addition, the electric compressor enables HEVs to shut off the engine during vehicle stops or at low vehicle speeds when the engine power is not required. Moreover, fuel cell powered vehicles require an electrically driven HVAC compressor.

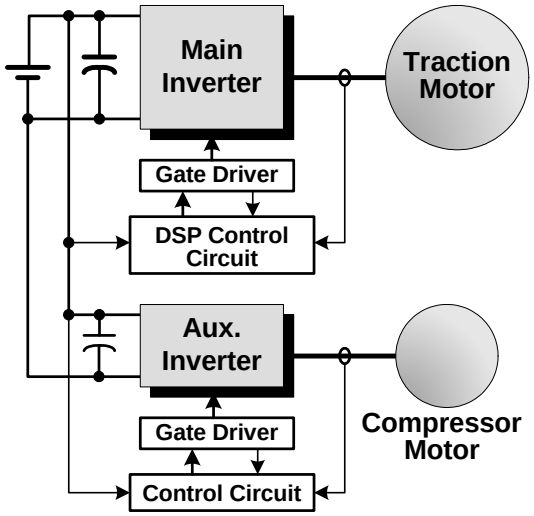

Fig. 1. A conventional traction and compressor motor drive configuration using two separate inverters.

Fig. 1 shows a conventional drive configuration where two separate inverters are used, one for the traction drive and the other for the compressor motor. While a typical compressor drive may employ a three-phase inverter and a three-phase motor as shown in Fig. 2(a), to reduce the cost, two-phase inverter-fed induction motor drives were used to replace wound-field or permanent magnet dc motors for heating, ventilating, demisting, engine-cooling, and water-pumping applications in the automotive industry [5–6]. Compared to the three-phase motor fed by a three-phase inverter, which typically requires six switches, a two-phase motor can be controlled by a lower cost two-leg inverter plus a split-capacitor leg as illustrated in Fig. 2(b). Unlike a semiconductor switch leg, the split-capacitor leg does not need additional gate drive or control circuits, thus making it cheaper than a semiconductor switch leg.

It is apparent that the number of components can be reduced by simply integrating the two-phase inverter into the three-phase main inverter, as shown in Fig. 3, because

* Prepared by Oak Ridge National Laboratory, managed by UT-Battelle, LLC, for the U.S. Dept. of Energy under contract DE-AC05-00OR22725. The submitted manuscript has been authored by a contractor of the U.S. Government under contract DE-AC05-00OR22725. Accordingly, the U.S. Government retains a nonexclusive, royalty-free license to publish or reproduce the published form of this contribution, or allow others to do so, for U.S. Government purposes.

the control circuit, dc bus filter capacitor, and possibly some of the gate drive power supplies can be shared. Electrolytic capacitors, while frequently used in industrial and commercial applications due to their volumetric efficiency and lower cost, have a low reliability and a short service lifespan, and thus are being replaced by film or ceramic capacitors in EV/HEV applications because of the harsh environments expected in those applications. Film and ceramic capacitors, however, are costly and have a large volume for the same amount of capacitance. It is therefore desirable to eliminate the split-capacitor leg.

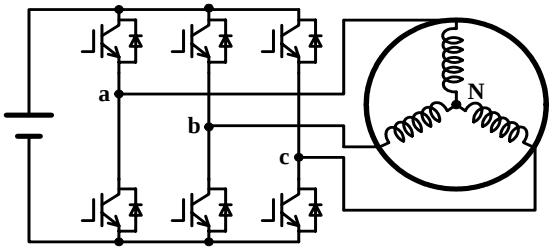

(a) A typical adjustable speed drive employing a three-phase inverter and motor.

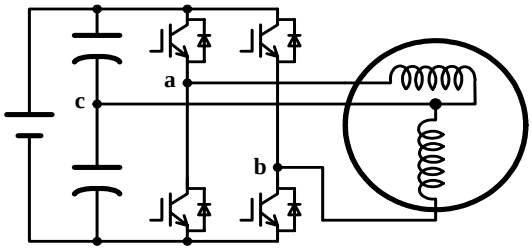

(b) A low-cost two-phase motor drive using four switches and two capacitors

Fig. 2. Adjustable speed drives for automotive HVAC compressor drive applications.

This paper presents an integrated traction and compressor drive to reduce the HVAC compressor drive cost for EV/HEV applications. The drive system employs a five-leg inverter to drive a three-phase traction motor and a two-phase compressor motor. The common terminal of the two-phase motor is tied to the neutral point of the three-phase traction motor to eliminate the requirement of a third phase-leg. The cost of the compressor drive can be significantly lowered due to the elimination of one phase leg and further part count reduction made possible by sharing the switching devices, dc bus filter capacitors, gate drive power supplies, and control circuit. Therefore, integrating the compressor drive into the traction motor drive results in a lower cost, smaller volume drive system. The proposed drive system was initially validated by testing results with an asymmetrical two-phase motor [7]. This paper includes extensive experimental results with a symmetrical two-phase motor to verify that speed control of the two motors is independent from each other.

II. Proposed Integrated Traction and Compressor Drive System

A. *Description of the Integrated Drive System*

Fig. 4 shows the proposed integrated drive system that employs a five-leg inverter for driving a three-phase traction motor and a two-phase compressor motor. The inverter consists of a dc source, V_{dc}, a filter capacitor, C_{dc}, and five phase-legs, *U*, *V*, and *W* for feeding the traction motor, *a* and *b* for the compressor motor. The two-phase motor has two orthogonal windings, phase-*a* and phase-*b*, and they are connected at one end to form a common terminal, T_{com}, with the other ends remaining separated to form two independent phase terminals, T_a and T_b.

The first three legs of the inverter, *U*, *V*, and *W* consisting of the switches S_1~S_6 form a three-phase main inverter, which through pulse width modulation (PWM) provides three sinusoidal currents to the three-phase motor. The remaining two legs, *a* and *b*, are connected to the independent phase terminals of the two-phase motor, T_a and

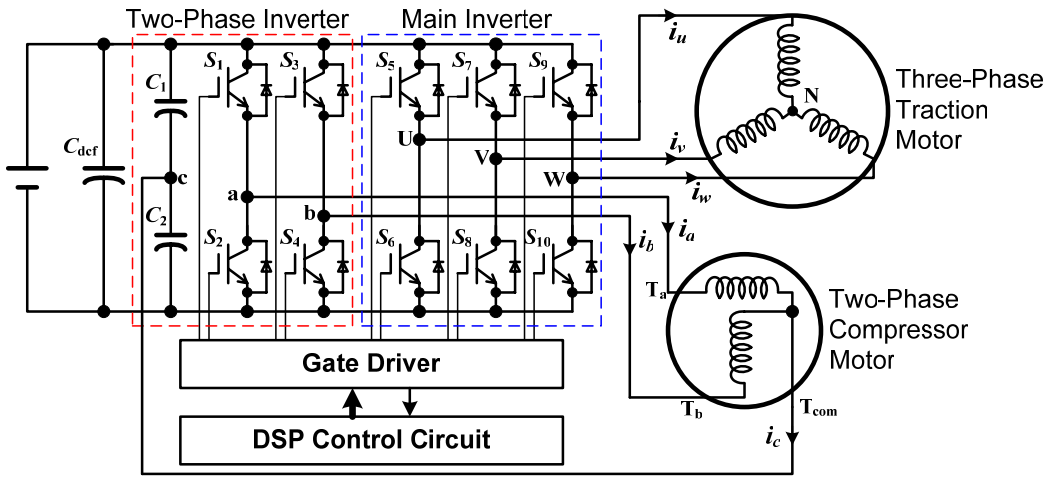

Fig. 3. A straightforward way for integrating the two-phase compressor drive into a three-phase traction motor drive system.

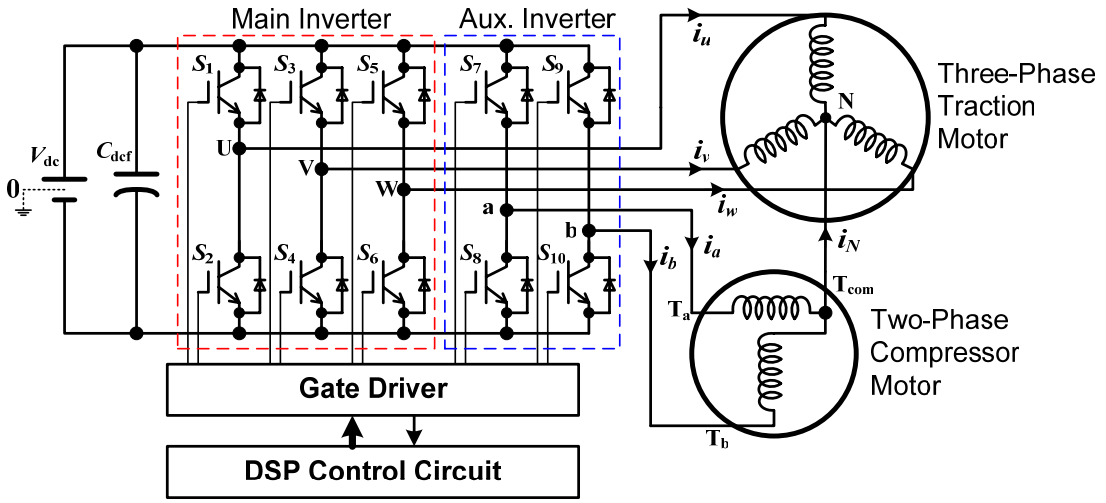

Fig. 4. Proposed integrated system for driving a three-phase traction motor and a two-phase compressor motor.

T_b, respectively, forming an auxiliary two-phase inverter. In addition, the common terminal, T_{com}, is connected to the neutral point, *N* of the three-phase motor to eliminate the need for a split-capacitor phase leg. The two phase-legs, *a* and *b*, by PWM, provide two sinusoidal currents with a phase shift of 90 electrical degrees to the two-phase motor. The sum of the two-phase currents, i_a and i_b, will return through the stator windings of the three-phase motor and the associated phase legs of the three-phase inverter.

It is apparent that by integrating the two-phase auxiliary inverter into the main three-phase inverter, the dc bus filter capacitor and gate drive power supplies for the bottom switches can be shared between the two inverters. In addition, a single control circuit typically based on a microprocessor or digital signal processor (DSP) with built-in motor control hardware such as A/D converters, PWM counters and encoder interface circuitry, can be used to execute control algorithms for the two motors. With a proper control algorithm, the motors can be run in either motoring mode, i.e., providing power to the motor shaft, or generating mode, in which power is transferred from the motor shaft to the inverter dc source.

B. Equivalent Circuits and Considerations of PWM Schemes

Fig. 5(a) shows an equivalent circuit of the integrated drive system, in which the inverter is represented by five voltage sources, v_u, v_v, v_w, v_a, and v_b, corresponding to the five phase-legs, *U*, *V*, *W*, *a*, and *b*, respectively. All the voltage sources are referred to the midpoint of the dc source, V_{dc}. By connecting the common terminal, T_{com}, to the neutral point, *N*, of the three-phase motor, the sum of the two-phase currents, i_N (= i_a + i_b), will split evenly into three parts and each part will flow through one of the phase windings of the three-phase motor and the associated phase leg of the three-phase inverter as the return paths, assuming

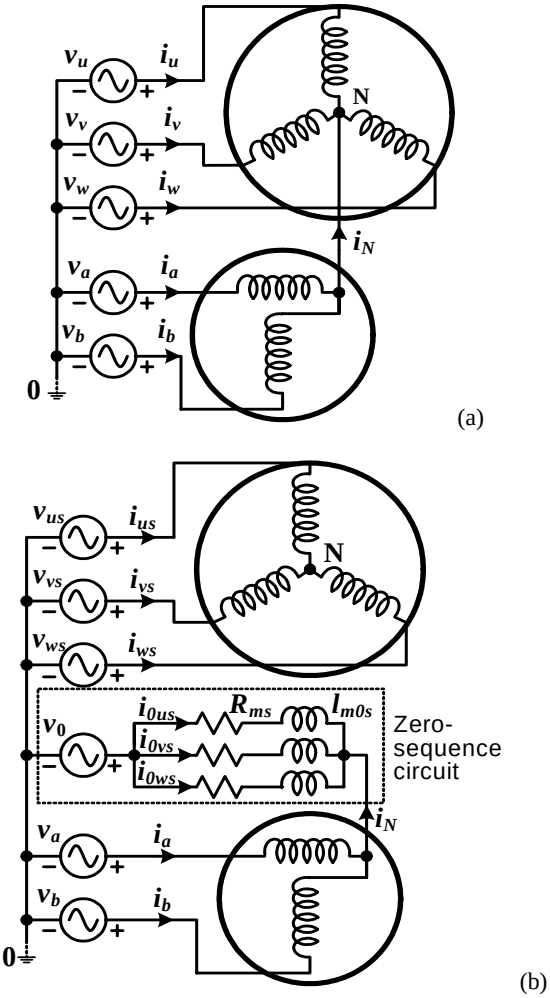

Fig. 5. Equivalent circuits; (a) showing inverter phase legs as voltage sources, and (b) showing the zero-sequence circuit of the main motor as the current return path of the two-phase motor.

a symmetrical three-phase motor and inverter. The two-phase motor currents are therefore zero-sequence

components flowing in the three-phase stator and will have no effect on the operation of the three-phase motor because the zero-sequence currents will not produce torque as shown in Fig. 5(b). In other words, the torque producing currents of the two motors can be controlled independently.

In Fig. 5(b), the zero-sequence circuit (ZSC) of the three-phase stator is separated from the positive and negative sequence circuits, where R_{ms} and l_{m0s} represent the resistance and inductance of the ZSC, and v_0 is the zero-sequence component of the three-phase voltage sources, v_u, v_v, and v_w, which may or may not exist depending on the PWM scheme. The zero-sequence voltage, v_0, can be calculated by:

$$v_0 = \frac{v_u + v_v + v_w}{3}. \tag{1}$$

v_{us}, v_{vs}, and v_{ws} are the phase voltages without the zero-sequence component of the three phases, *U*, *V*, and *W*, respectively, and are expressed by

$$\begin{cases} v_{us} = v_u - v_0 \\ v_{vs} = v_v - v_0 \\ v_{ws} = v_w - v_0 \end{cases}. \tag{2}$$

The zero-sequence voltage component, v_0, which could be generated by certain PWM strategies such as the space vector modulation schemes [8], can be cancelled by injecting the same component into the modulation signals for the two-phase inverter so that v_0 will not produce current in the circuit, as will be shown in the experimental results. Fig. 6 shows a conceptual block diagram to implement the cancellation method. The zero-sequence component, v_0, can be extracted from the three-phase modulation signals, v_{um}, v_{vm}, and v_{wm}, which are produced by the pulse width modulator based on the three-phase voltage references, v_{uref}, v_{vref}, and v_{wref}, and are added to the two-phase reference voltages, v_{aref} and v_{bref}. Therefore, the same zero-sequence voltage appears on all five phase voltages; canceling each other.

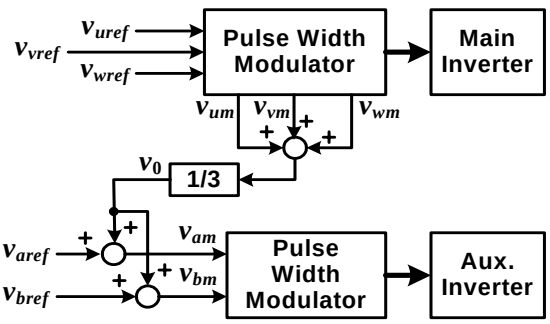

Fig. 6. PWM scheme for zero-sequence component cancellation.

C. *Effect on the Current Rating of the Main Motor due to the Two-Phase Motor Current*

Because the stator windings of the three-phase motor are utilized as the current return paths of the two-phase motor, the stator current rating may need to be increased to accommodate the two-phase motor currents. However, the increase of the main motor current is negligible if the two-phase motor current is sufficiently small compared to that of the main motor, which is typical in the intended automotive applications as shown below.

The phase current of the main motor, taking phase-*U* for example, i_u can be expressed by

$$i_u = i_{us} - \frac{i_a + i_b}{3}, \tag{3}$$

where i_{us} is the required current if the three-phase motor is operated alone without connection to the two-phase motor. Because the two motor currents will usually have different frequencies, the rms value of the main motor phase current, i_u, can therefore be calculated by

$$I_{u,rms} = \sqrt{I_{us,rms}^2 + \frac{2I_{a,rms}^2}{9}}, \tag{4}$$

where $I_{a,rms}$ is the required rms current of the two-phase motor. For instance, given a 350 Arms traction motor and a 25 Arms compressor motor, i.e., $I_{us,rms}$=350A and $I_{a,rms}$=25A, the resulting traction motor current is 350.2A, a negligible increase of less than 0.06%.

III. Experimental Results

Extensive testing was conducted to verify the proposed integated drive operations.

A. *Experimental Setup*

For testing, a 15 HP, 230/460V, six-pole, three-phase induction motor was used as the traction motor. The motor has two sets of stator windings that can be connected in series for 460V or in parallel for 230V operation in Δ connection. All winding terminals are accessible because it is intended to use a Y connection for starting and then a Δ connection for normal run. In our testing, each winding set is wired as a Y connection and then the two sets are connected in parallel to reduce the dc bus voltage requirement. For the compressor motor, a 3 HP, 230/460V, three-phase, four-pole motor, which also has two sets of stator windings, was rewound into a two-phase motor. To reduce the dc bus voltage requirement, the two sets of windings are also connected in parallel. The rated current and torque are 22 A and 90 N·m for the three-phase motor,

and 13 A and 12.5 N·m for the two-phase motor, respectively. Fig. 7 shows photos of the main motor mounted on a 100 HP dynamometer test bed and the two-phase motor connected to a hysteresis dynamometer.

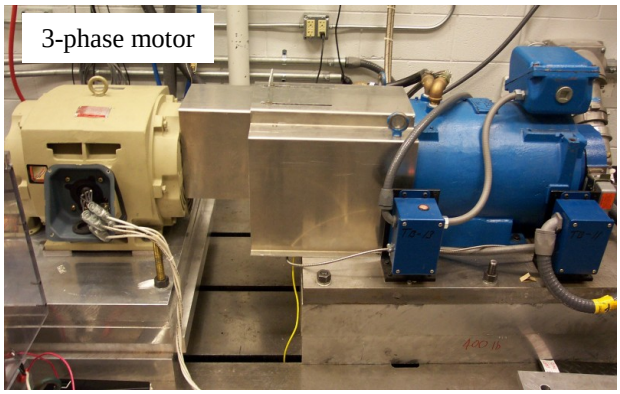

(a) Main motor mounted on a 100 HP dynamometer test bed

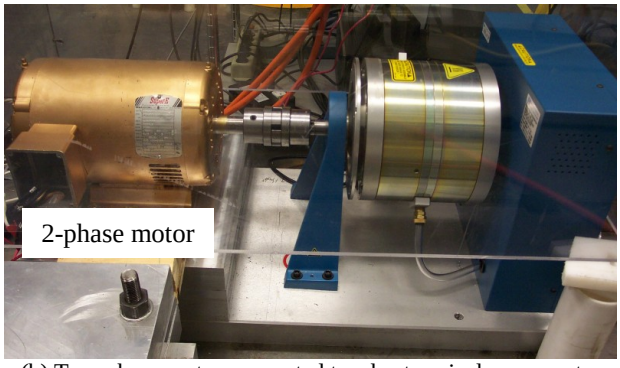

(b) Two-phase motor connected to a hysteresis dynamometer

Fig. 7. Photos of the motor testing setup.

B. *Experimental Results*

Fig. 8(a) – (g) give testing waveforms at various load conditions and without the zero-sequence components in the three-phase voltages, i.e. v_0=0, which clearly shows that the speed of the two motors can be controlled independently. In (a), the main motor was not running while the two-phase motor was loaded with 14.6 N·m at 1000 rpm, clearly showing that the neutral current is divided evenly over the three-phase conductors. In (b), the main motor was loaded with 90 N·m at 685 rpm and the two-phase motor was not running. In (c), the main motor was loaded with 90 N·m at 685 rpm while the two-phase motor ran at 750 rpm with no load. In (d), the main motor ran at 700 rpm with no load, while the two-phase motor was loaded with 9.5 N·m at 1000 rpm. In (e), the main motor was loaded with 85 N·m at 550 rpm; two-phase motor was loaded with 11 N·m at 1000 rpm. In (f), the main motor was loaded with 90 N·m at 685 rpm, while the two-phase motor was loaded with 14.9 N·m at 750 rpm. In (g) the main motor was loaded with 90 N·m at 685 rpm, while the two-phase motor was loaded with 14.8 N·m at 1100 rpm. It should be noted that the main motor was tested with a limited speed range because at the dc bus voltage of 350 V the inverter can not produce the rated motor voltage of 400 V, and the dynamometer, which has a maximum speed of 10,000 rpm, could not stably load the motor at speeds under 500 rpm.

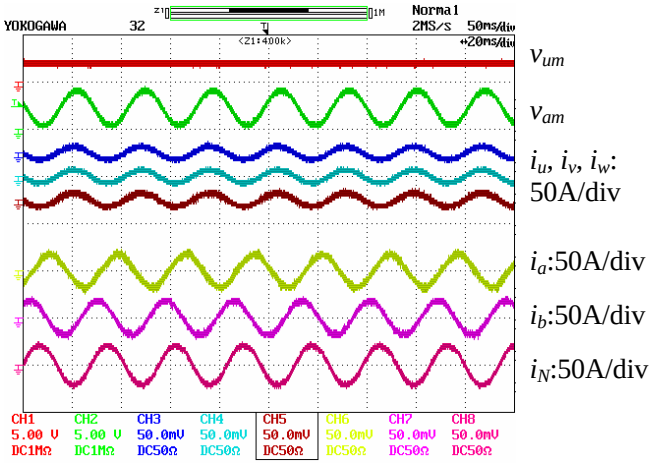

(a) Main motor is not running while two-phase motor is loaded with 14.6 N·m at 1000 rpm. Time: 20ms/div.

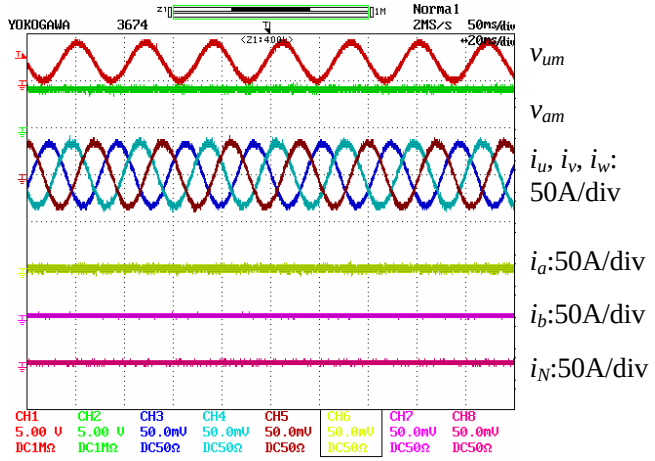

(b) Main motor is loaded with 90 N·m at 685 rpm, while two-phase motor is not running. Time: 20ms/div.

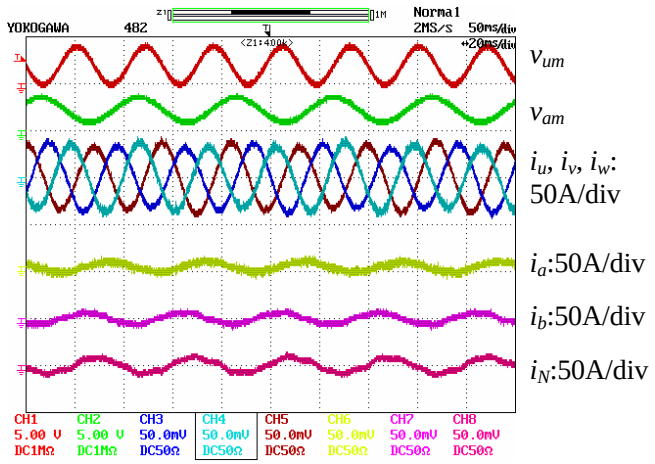

(c) Main motor is loaded with 90 N·m at 685 rpm with unloaded two-phase motor at 750 rpm. Time: 20ms/div.

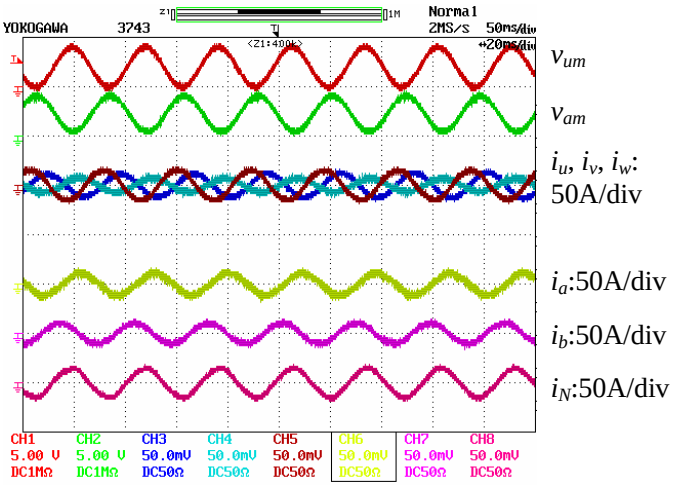

(d) Main motor at 700 rpm, no load, Two-phase motor loaded with 9.5 N·m at 1000 rpm. Time: 20ms/div.

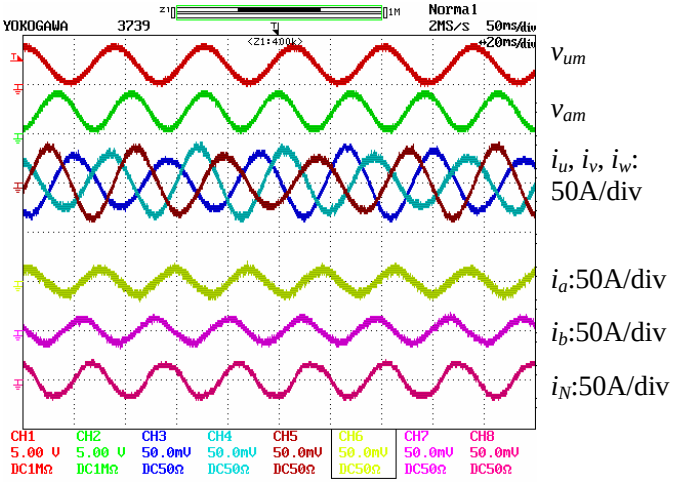

(e) Main motor loaded with 85 N·m at 550 rpm, two-phase motor loaded with 11 N·m at 1000 rpm. Time: 20ms/div.

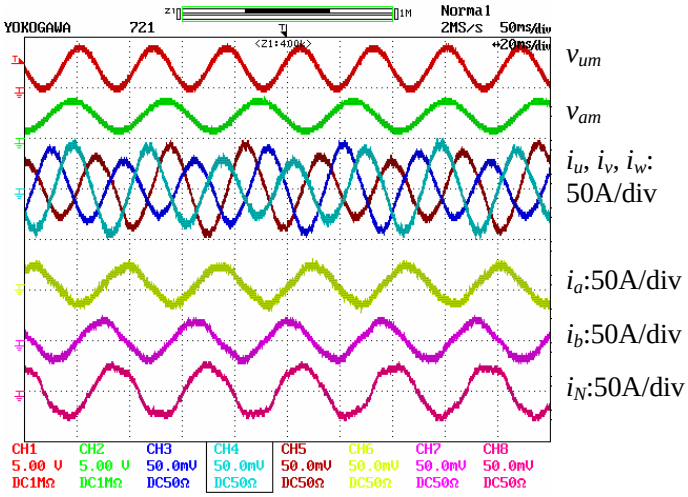

(f) Main motor loaded with 90N·m at 685 rpm, two-phase motor loaded with 14.9 N·m at 750 rpm. Time: 20ms/div.

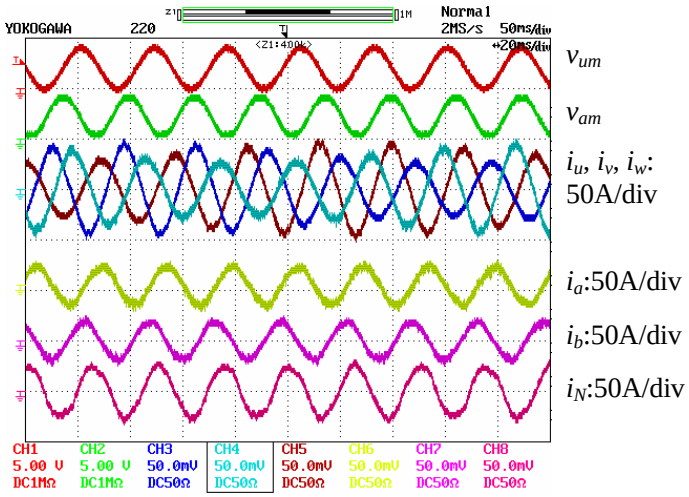

(g) Main motor loaded with 90 N·m at 685 rpm, two-phase motor loaded with 14.8 N·m at 1100 rpm. Time: 20ms/div.

Fig. 8. Testing waveforms at various load conditions showing that the speed of the two motors can be controlled independently.

With the space vector based PWM schemes, a third harmonic current was generated as shown in Fig. 9 (a) before turning on the zero-sequence voltage cancellation in the two-phase inverter. The source was three-phase modulation signals containing triplet harmonics, which are zero-sequence components, i.e. $v_0 \neq 0$. In Fig. 9(a), the unloaded main motor was running at 700 rpm and the unloaded two-phase motor at 500 rpm. By adding the same triplet harmonics to the two-phase modulation signals, v_{am} and v_{bm}, no third harmonic current was produced as illustrated in Fig. 9(b).

IV. CONCLUSIONS

The proposed integrated traction and compressor motor drive using a five-leg inverter can significantly reduce the cost of the compressor motor drive in EV/HEV applications. The experimental results show that:

- The split-dc bus capacitors for a two-phase compressor motor drive can be eliminated by using the traction motor stator windings as the current return paths.
- Increase in the current rating of the main inverter switches and the traction motor due to the two-phase motor current is negligible.
- Speed of the traction and compressor motors can be controlled independently from each other. The test results on the independent control characteristics of the two motors and on the voltage waveforms agree fully with the analytical predictions.
- The fundamental voltage and current components of the two motors have no influence on each other.

While induction motors are discussed in this paper, the proposed inverter is applicable to ac synchronous permanent magnet machines and brushless dc motors.

REFERENCES

[1] H. Murakami, H. Kataoka, and Y. Honda, "Highly Efficient Brushless Motor Design for an Air-conditioner of the Next Generation 42V Vehicle," *Proceedings of the Industry Applications Society Annual Meeting*, Chicago, Oct. 2001, pp. 461-466.

[2] P. J. McCleer, "Electric Drives for Pump, Fan and Compressor Loads in Automotive Applications," *Proceedings of the Industry Applications Society Annual Meeting*, 1995, pp. 80-85.

[3] J. L. Oldenkemp and D. M. Erdman, "Automotive Electrically Driven Air-conditioning System," *Automotive Power Electronics*, Aug. 1989, pp. 71-72.

[4] J. Kiekmann and D. Mallory, "Variable Speed Compressor HFC-134A Based Airconditioning System for Electric Vehicles," *SAE* Paper 920444.

[5] I. R. Smith, G. Creighton, and L. M. C. Mhango, "Analysis and Performance of a Novel Two-Phase Drive for Fan and Water-Pumping Applications," *IEEE Trans. Industrial Electronics*, vol. 36, no. 4, pp. 530–538, Nov. 1989.

[6] F. Blaabjerg, F. Lungeanu, K. Skaug, and M. Tonnes, "Evaluation of Low-cost Topologies for Two Phase Induction Motor Drives in Industrial Applications," *Conf. Rec. 37th IEEE/IAS Ann. Meeting*, vol. 4, pp. 2358–2365, Oct. 2002.

[7] G. J. Su and J. S. Hsu, "A Five-Leg Inverter for Driving a Traction Motor and a Compressor Motor," the 8th IEEE Workshop on Power Electronics in Transportation (WPET2004), pp. 117–123, Oct. 21-22, 2004, Novi, Michigan, USA.

[8] J. Holtz, "Pulsewidth Modulation for Electronic Power Conversion," *Proc. IEEE*, vol. 82, pp. 1194–1214, Aug. 1994.

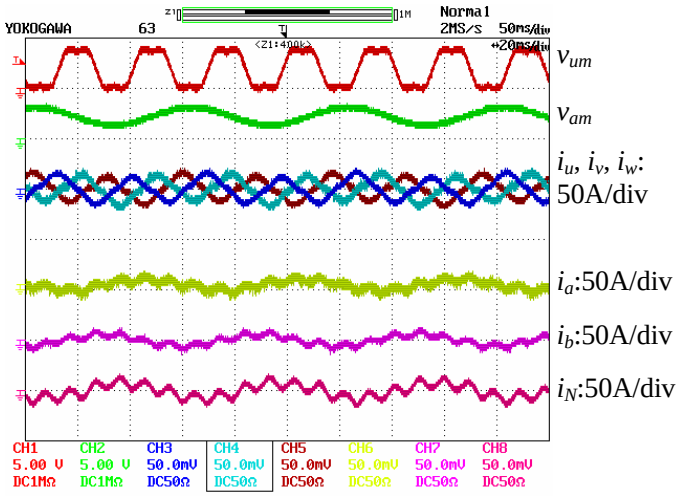

(a) Without the zero-sequence voltage cancellation. Main motor at 700 rpm, two-phase motor at 500 rpm, no load. Time: 20ms/div.

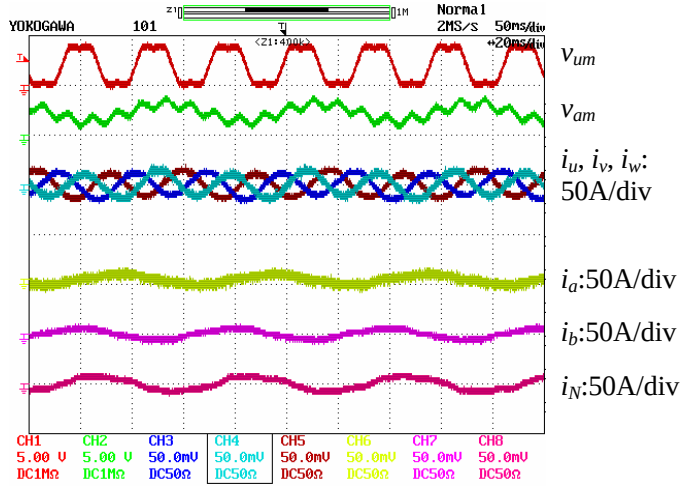

(b) With the zero-sequence voltage cancellation. Main motor at 700 rpm, two-phase motor at 500 rpm. Time: 20ms/div.

Fig. 9. Testing waveforms showing that third harmonic components in the three-phase voltages can be prevented from producing current.